



## **Thermally Induced Polymorphic Transformation of Hexanitrohexaazaisowurtzitane (HNIW) Investigated by *in-situ* X-ray Powder Diffraction**

Yu LIU,<sup>1,2</sup> Shichun LI,<sup>2</sup> Zeshan WANG,<sup>1</sup> Jinjiang XU,<sup>2\*</sup>  
Jie SUN,<sup>2</sup> Hui HUANG<sup>2</sup>

<sup>1</sup> *School of Chemical Engineering,  
Nanjing University of Science & Technology,  
Nanjing 210094, People's Republic of China*

<sup>2</sup> *Institute of Chemical Materials,  
Chinese Academy of Engineering Physics (CAEP),  
Mianyang 621900, People's Republic of China*

\**E-mail: xjxujinjiang@126.com*

**Abstract:** The  $\varepsilon \rightarrow \gamma$  phase transition of HNIW induced by heat was investigated with *in situ* X-ray powder diffraction (PXRD). The effects of purity, particle size, insensitive additives and the time of isothermal heat treatment on the phase transition were evaluated. It was found that the phase transition is irreversible with changes in temperature, and the two phases can coexist in a certain temperature range. Moreover, the initial phase transition temperature increases with increasing purity and decreasing particle size of HNIW, and thus with the approximate crystal density. The addition of graphite and paraffin wax to HNIW as insensitive additives leads to a decrease in the initial phase transition temperature, but the addition of TATB does not affect the initial phase transition temperature. Thus, TATB is a suitable insensitive additive. Moreover, at the critical temperature, the isothermal time determined the efficiency of the  $\varepsilon$ - to  $\gamma$ -phase transition. This work lays the foundations for the choice of molding technologies, performance test methods, ammunition storage options, as well as the manufacture of HNIW-based explosive formulations.

**Keywords:** HNIW, polymorphism, *in situ* X-ray diffraction, phase transition, heat stimulation

## 1 Introduction

Polymorphism, defined as the ability of a material to crystallize in different crystal structures, is frequently encountered in organic crystals. Polymorphic crystals have the same structure in the liquid and gaseous states, but different structures and physicochemical properties in the solid state. The different properties include solubility, density, morphology, melting point, stability and so on, which have significant effects on the industrial processing and applications of the materials [1, 2]. For instance, in the field of energetic materials, the density of an explosive strongly affects the detonation performance, including the detonation velocity, pressure, heat, *etc.* [3, 4]. Owing to the differences in density and stability between polymorphs, the energy output and detonation performance are dependent on polymorphism. Therefore, to satisfy the requirement of high energy density, energetic materials with high density and a stable structure have to be prepared. The polymorphic transformation kinetics of an explosive could be affected by many factors, such as temperature, solvent, pressure, and additives, and have been of serious concern to the energetic materials industry [5-7].

2,4,6,8,10,12-Hexanitro-2,4,6,8,10,12-hexaazaisowurtzitane (HNIW, also called CL-20) was firstly synthesized in 1987 by A. T. Nielsen, an American chemist at the Naval Weapons Center, China Lake [8, 9]. HNIW possesses a very high energy density due to the ratio of carbon atoms to nitro groups (1:1) and the highly strained molecular cage structure (Figure 1). Thus, HNIW shows potential for wide spread use in many munitions applications. The different extended orientations of the nitro groups relative to the five- or six-membered rings of HNIW leads to different molecular packing models and different numbers of molecules in a cell, which defines several probable polymorphs of HNIW. So far, five different polymorphs ( $\alpha$ ,  $\beta$ ,  $\gamma$ ,  $\epsilon$ , and  $\zeta$ ) have been reported and identified [10-14]. Four of the polymorphs ( $\alpha$ ,  $\beta$ ,  $\gamma$ , and  $\epsilon$ ) exist at ambient pressure and temperature. Only  $\epsilon$ -HNIW is applied in practice because of its good thermal stability and the highest energy density [15-18] (theoretical density of  $2.044 \text{ g}\cdot\text{cm}^{-3}$  [19]).

However, the  $\epsilon$ -phase can be converted to other phases under extreme conditions [20]. Heat is an important factor promoting the reconstruction of  $\epsilon$ -HNIW. Russell [5, 12] investigated the effects of temperature and pressure on the solid-state phase transition of HNIW by DSC and found that  $\alpha$ ,  $\beta$ , and  $\epsilon$ -form could transform to  $\gamma$ -HNIW when heated. Turcotte [21] reported that at a temperature of 160-170 °C, a solid-solid phase transition of  $\epsilon \rightarrow \gamma$  polymorphs occurs in HNIW. They proposed that the transition temperature was related to the crystal quantity of HNIW. Moreover, the potential use of HNIW in TNT/ETPE

based melt cast formulations was investigated by Thiboutot [22]. It was found that molten TNT could partially dissolve  $\epsilon$ -HNIW followed by phase transition to  $\beta$ -HNIW, resulting in a decrease in charge density and an increase in sensitivity. These phase transitions of HNIW lead to a decrease in thermal stability and detonation power, which reduces the safe performance of weapons and affects the application of HNIW. Therefore, a study of the evolution characteristics and influential factors on the phase transition of  $\epsilon$ -HNIW has practical significance.

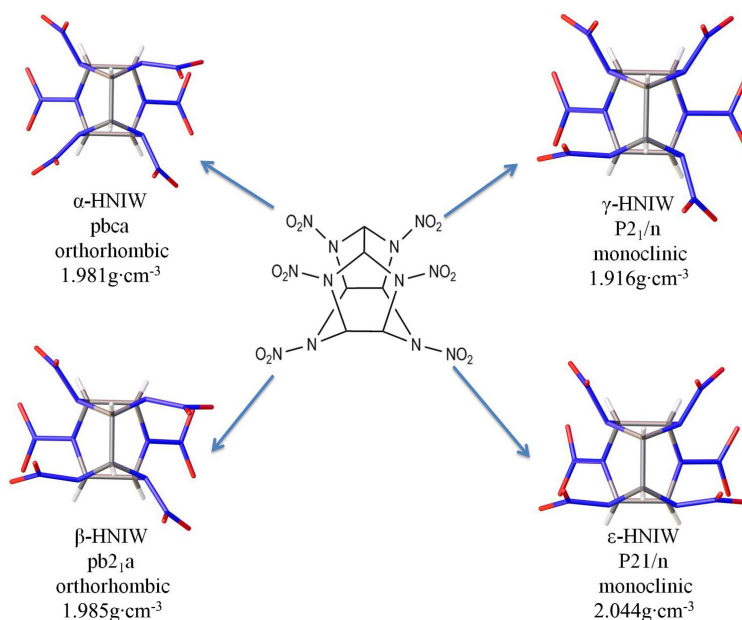


**Figure 1.** Molecular structures of HNIW and its different conformers which form  $\alpha$ -,  $\beta$ -,  $\gamma$ -, and  $\epsilon$ -HNIW.

In the present work, the evolution of HNIW was investigated with *in-situ* PXRD under heat stimulation. The aim of the work was to study the effects of purity, particle size, insensitive additives and the time of isothermal heat treatment on solid-solid phase transitions. This work provides new insights into the solid-state phase transitions of HNIW, and is significant for controlling the polymorphic form of HNIW and maintaining the pure form in applications.

## 2 Experimental

### 2.1 Materials and instruments

HNIW was synthesized by Qingyang Chemical Industry Corporation in China and recrystallized by evaporation from ethyl acetate before use. Insensitive additives such as 1,3,5-triamino-2,4,6-trinitrobenzene (TATB), graphite, and paraffin wax were produced by the Institute of Chemical Material, China Academy Engineering Physics.

X-ray powder diffraction (PXRD) analysis was performed on a Bruker D8 Advance X-ray powder diffractometer by using Cu K $\alpha$  radiation without a monochromator. An Anton Paar TTK 450 temperature chamber was used as the heating device during the experiments and the temperature uncertainty was 0.1 °C. The X-ray tube operating conditions were set at 40 kV and 40 mA, while a Vantec-1 detector was adopted during the experiments. Samples were packed into a metallic holder and scanned from 5° to 50° in 2 $\theta$ , increasing in increments of 0.02°; the counting time was set at 0.1 s per increment. The purity was determined by high performance liquid chromatography (HPLC, Agilent Series 220). The particle size distribution was measured with a Beckman Coulter LS230. The apparent density of the sample was measured with a home-made density gradient apparatus [23, 24]. Aqueous ZnBr<sub>2</sub> solution as the gradient liquid was in the density gradient column.

### 2.2 Temperature programme

A series of PXRD detections was performed at different temperatures controlled by the programme. The rate of temperature change was 0.1 °C/s, and scanning was performed at 5 min after the target temperature had been reached. Firstly, the temperature was raised from ambient to 30 °C, and scanning data was collected. After that, the temperature was increased to 125 °C and a second scanning process was carried out. Then, the temperature was increased to 180 °C, and scanning was performed at 5 °C intervals. After the scanning process at 180 °C, the temperature was decreased to 30 °C, and the final scanning process was carried out. The uncertainty of the initial phase transition temperature determined by the *in-situ* variable temperature PXRD patterns was 5 °C.

### 2.3 Rietveld method

The Rietveld refinement method was used to calculate the phase content of the HNIW crystals through the Topas Academy program, which is a standardless X-ray diffraction, quantitative phase analysis method of the complete powder diffraction pattern. Based on the Rietveld method [25, 26], the weight fraction

$\omega$  for each phase is related to the overall Rietveld scale factor  $S$ . The calculated intensities  $y_{ci}$  in the  $2\theta_i$  position and the weight fraction of phase  $\gamma$  in an  $n$  phase mixture are given by the relationships:

$$y_{Ci} = \sum_j S_j \sum_{jK} L_{jK} |F_{jK}|^2 \phi_{iK} (2\theta_{ji} - 2\phi_{jK}) P_{jK} A_j + Y_{bi} \quad (1)$$

$$\omega_\gamma = \frac{S_\gamma (ZMV)_\gamma}{\sum_{j=1}^n S_j (ZMV)_j} \quad (2)$$

where  $S$  is the scale factor,  $K$  represents the Miller indexes  $hkl$  for a Bragg reflection,  $L_K$  contains the Lorentz, polarization and multiplicity factors,  $\Phi$  is the reflection profile function,  $P_K$  is the preferred orientation function,  $A$  is an absorption factor,  $F_K$  is the structure factor for the  $K^{\text{th}}$  Bragg reflection and  $Y_{bi}$  is the background intensity at the  $i^{\text{th}}$  step. In Equation 2,  $(ZMV)_\gamma$  is the “calibration constant” for phase  $\gamma$  and can be calculated from published or refined crystal structure information alone ( $Z$  is the number of formula units in the unit cell,  $M$  is the molecular mass of the formula unit,  $V$  is the unit cell volume). The scale factor  $S$  is a multiplier for each phase contribution to the whole powder pattern, which is related to the relative abundance of that phase and can be calculated from Equation 1.

### 3 Results and Discussion

#### 3.1 *In-situ* X-ray powder diffraction analysis

The XRD patterns of standard  $\varepsilon$ - and  $\gamma$ -HNIW covering  $2\theta$  from  $5$  to  $50^\circ$  are shown in Figure 2. The crystallographic parameters are referred from the refcode PUBM002 [27] and PUBM001 [27] of the Cambridge Structural Database (CSD) [28]. Considerable differences exist between the patterns and can be used to distinguish the polymorphs of HNIW. For example, a strong peak appeared at the  $2\theta$  position of ca.  $13^\circ$ , which belongs to  $\gamma$ -HNIW.

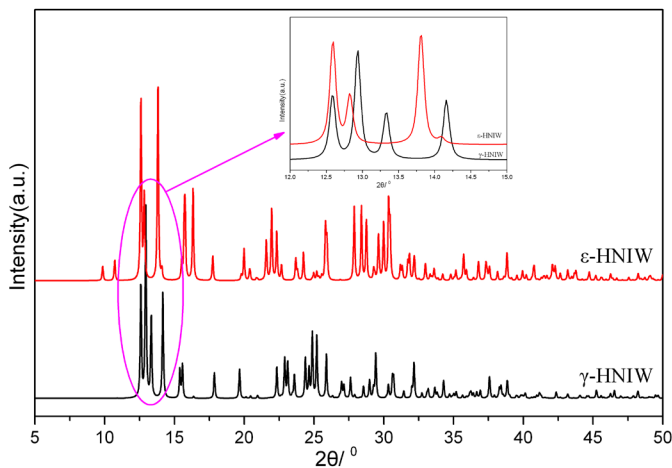


**Figure 2.** XRD patterns of  $\epsilon$ -, and  $\gamma$ -HNIW crystals. In the inset the characteristic peaks of  $\epsilon$  ( $12.82^\circ$  and  $13.82^\circ$ ,  $2\theta$ ) and  $\gamma$  ( $12.94^\circ$ ,  $13.36^\circ$  and  $14.16^\circ$ ,  $2\theta$ ) are indicated from  $12^\circ$  to  $15^\circ$ . These were used to estimate the change of the patterns when heating.

Figure 3 shows the XRD patterns of the  $\epsilon$ - to  $\gamma$ -HNIW phase transition at elevated temperature. The samples of  $\epsilon$ -HNIW possessed chemical purity of 99.6%, particle size distribution of 75~125  $\mu\text{m}$  and an average apparent density of  $2.0374 \text{ g}\cdot\text{cm}^{-3}$  at  $23^\circ\text{C}$ . As shown in Figure 3, the diffraction patterns consist of pure  $\epsilon$ -phase peaks below  $150^\circ\text{C}$  and a new weak phase peak is found at  $13.36^\circ 2\theta$  at  $155^\circ\text{C}$ . Compared with the XRD patterns of standard  $\gamma$ -HNIW, this particular peak is attributed to the  $\gamma$ -phase. With increasing temperature, the intensity of the peak at  $13.36^\circ$  increases, while the characteristic peak of  $\epsilon$ -HNIW at  $10.70^\circ 2\theta$  becomes weaker. The results indicate that the proportion of the two kinds of polymorph has changed. The quantitative determination data of the mixture by Rietveld refinement were 85.5% of  $\epsilon$ -HNIW and 14.5% of  $\gamma$ -HNIW at  $155^\circ\text{C}$  through the Topas software of the Bruker Company [29]. The error in the Rietveld refinement was less than 3% in this work due to the high purity and narrow particle size distribution of the samples and careful collection of the pattern data [30-33]. When the temperature rose to  $180^\circ\text{C}$ , the main component of the mixture was  $\gamma$ -HNIW (about 89.5%). The results show that the phase transition occurs without complete destruction of the  $\epsilon$ -phase. In the temperature range of  $150^\circ\text{C}$  to  $180^\circ\text{C}$ , the two phases can coexist, and can be used for kinetics research. In addition, it was found that the phase transition is irreversible on cooling.

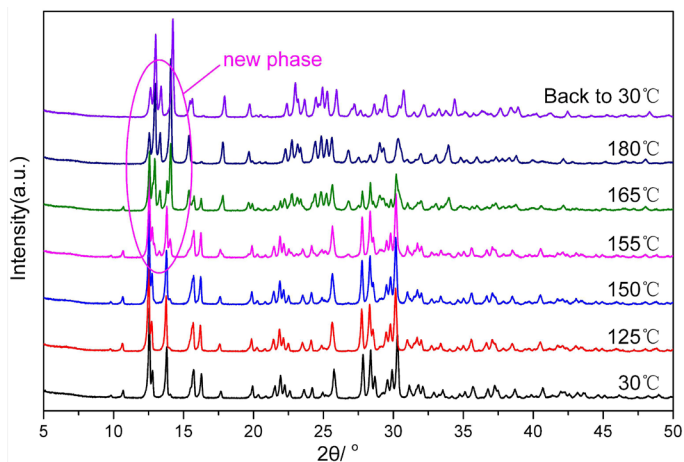


**Figure 3.** XRD patterns of the  $\epsilon$ - to  $\gamma$ -HNIW phase transition at elevated temperature. The characteristic peaks from  $12^\circ$  to  $15^\circ$  show distinct differences on heating and the appearance of new peaks were used to estimate the initial polymorphic transition temperature. The highlighted area shows the presence of the  $\gamma$ -form in the sample.

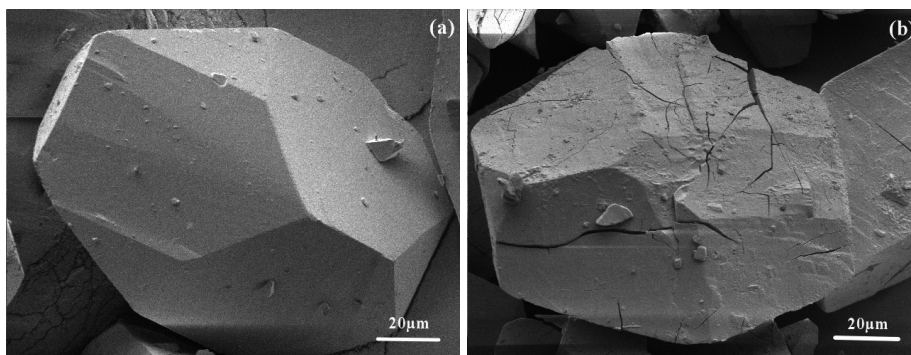


**Figure 4.** Morphological change of HNIW induced by heating: (a) before phase transition, (b) after phase transition.

Along with the morphological change of  $\epsilon$ -HNIW, it can be seen (Figure 4; before and after polymorphic transformation) that obvious cracks appeared on the surface of the crystals. Although  $\epsilon$ - and  $\gamma$ -HNIW both belong to the monoclinic system and have the same space group ( $P2_1/n$ ), the crystal structures such as nitro orientation and lattice parameters are different. The unit cell volume of the  $\gamma$ -crystal form ( $1.519 \text{ nm}^3$ ) is larger than that of the  $\epsilon$ -form ( $1.424 \text{ nm}^3$ ), and results in volume expansion of the crystal after the thermally induced

phase transition. Thus, in the macroscopic view, the density of the  $\gamma$ -form ( $1.916 \text{ g}\cdot\text{cm}^{-3}$ ) is less than that of the  $\varepsilon$ -form ( $2.044 \text{ g}\cdot\text{cm}^{-3}$ ). According to hotspot theory [34], the defects can lead to an increase in the mechanical sensitivity of the explosive and a decrease in safety, and thus could not fulfill the requirements for weapons applications.

### 3.2 Influence of purity on crystal structural transformation

The purity of the sample is an important parameter in a quality judgment of HNIW, because the purity strongly affects the physicochemical properties [35]. *In-situ* PXRD experiments were conducted to investigate the influence of purity on the  $\varepsilon \rightarrow \gamma$  phase transition. The results are given in Table 1.

**Table 1.** Initial phase transition ( $\varepsilon \rightarrow \gamma$ ) temperature of HNIW with different chemical purities

Sample	Initial polymorph	Average particle size [ $\mu\text{m}$ ]	Mean density [ $\text{g}\cdot\text{cm}^{-3}$ ]	Chemical purity [%]	Initial phase transition temperature [ $^{\circ}\text{C}$ ]
crys-1	$\varepsilon$	65.2	2.0309	94.2	145
recrys-1	$\varepsilon$	59.7	2.0324	95.5	150
recrys-2	$\varepsilon$	62.3	2.0334	96.4	150
recrys-3	$\varepsilon$	59.5	2.0349	98.3	155
recrys-4	$\varepsilon$	55.7	2.0382	99.6	160

It can be seen that the initial phase transition temperature increases with increasing purity of the samples (note: if a lower temperature gradient is utilized, more accurate initial phase transition temperatures could be obtained). This is attributed to the presence of impurities reducing the energy barrier for phase transition, and the heat accumulation and energy release of impurities providing additional energy to promote the phase transition [10, 11]. Therefore, purity is a key factor in ensuring the stability and safety of HNIW.

### 3.3 Influence of particle size on crystal structural transformation

In order to investigate the influence of various particle sizes on the phase transition of HNIW, four samples with particle size distributions of 5-25  $\mu\text{m}$ , 45-75  $\mu\text{m}$ , and 150-250  $\mu\text{m}$ , together with a ground sample of the latter, were selected for *in-situ* PXRD experiments. The samples possessed similar chemical purities, *i.e.* 99.6, 99.6 and 99.5%, and similar average density, *i.e.* 2.0386, 2.0378 and 2.0372  $\text{g}\cdot\text{cm}^{-3}$ . Figure 5 shows the XRD patterns of the  $\varepsilon$ - to  $\gamma$ -HNIW phase transition with different particle size distributions.



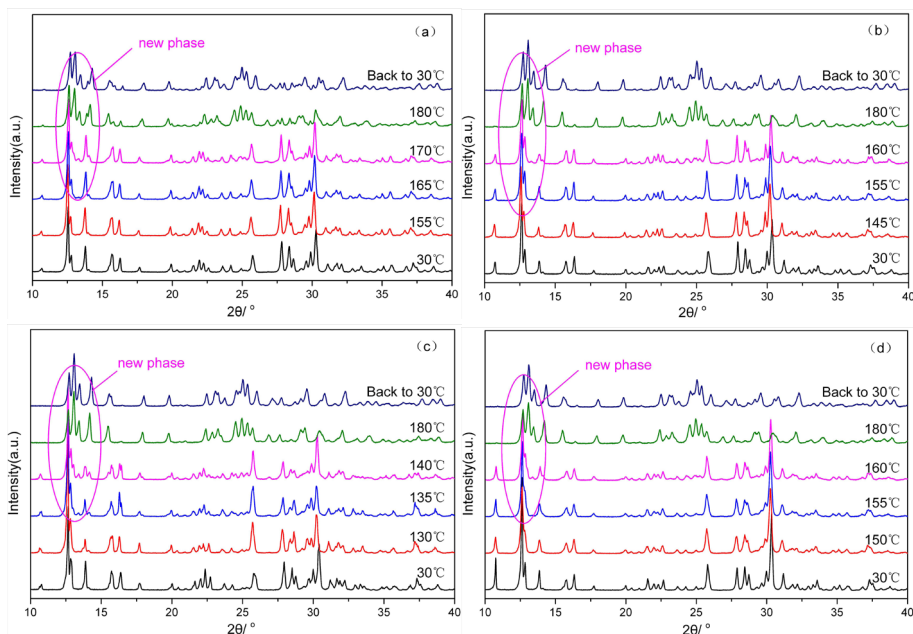


**Figure 5.** XRD patterns of the  $\epsilon$ - to  $\gamma$ -HNIW phase transition with different particle size distributions: (a) 5-25  $\mu\text{m}$ ; (b) 45-75  $\mu\text{m}$ ; (c) 150-250  $\mu\text{m}$ ; (d) sample c (150-250  $\mu\text{m}$ ) was ground in an agate mortar. The new characteristic peaks of  $\gamma$ -HNIW from  $12^\circ$  to  $15^\circ$  appeared in the highlighted area when heated, indicating that the  $\epsilon$ -phase had begun to transform to the  $\gamma$ -phase. The initial phase transition temperature was different when the particle size of HNIW was increased.

In theory, a sample with a smaller particle size has a larger surface area, higher surface energy and higher surface activity [36]. Thus, the crystal structural transformation should appear at a lower temperature. However, an unusual phenomenon was observed in Figure 5. The initial phase transition temperature decreased with increasing particle size. As shown in Figures 5a, 5b and 5c, the initial phase transition temperatures of the samples were about  $165^\circ\text{C}$ ,  $155^\circ\text{C}$  and  $135^\circ\text{C}$  with the particle size distributions of 5-25  $\mu\text{m}$ , 45-75  $\mu\text{m}$  and 150-250  $\mu\text{m}$ , respectively. The differences in the initial phase transition temperatures may be caused by the following. Firstly, the loading density of HNIW with larger particle size is lower than with the smaller one, so less energy is needed to realize the phase transition. Secondly, the HNIW with larger particle sizes possesses more crystal defects, such as internal void and solvent, confirmed by the densities, which increases the speed of crystal reconstruction in the phase transition and

reduces the energy barrier required. Figure 5d confirms that the initial phase transition temperature with particle size distribution of 150-250  $\mu\text{m}$  increased to about 155  $^{\circ}\text{C}$  after grinding.

### 3.4 Influence of insensitive additives on crystal structural transformation

Compared with the ordinary nitramine explosives such as octahydro-1,3,5,7-tetranitro-1,3,5,7-tetrazocine (HMX) and hexahydro-1,3,5-trinitro-1,3,5-triazine (RDX), the safety performance of HNIW should be improved on being applied in the formulation design of a composite explosive. In general, insensitive additives are used to reduce the sensitivity of individual explosives [37]. In order to investigate the influence of different insensitive additives on the  $\varepsilon \rightarrow \gamma$  phase transition, the sample with the particle size distribution of 5-25  $\mu\text{m}$ , average density of  $2.0386 \text{ g}\cdot\text{cm}^{-3}$  and purity of 99.57%, was mixed with different insensitive additives in different proportions. TATB and graphite were mixed with HNIW by dry blending, and a mixture of wax and HNIW was prepared by dispersing HNIW in a chloroform solution of wax and then evaporating the chloroform. The results are shown in Figure 6.

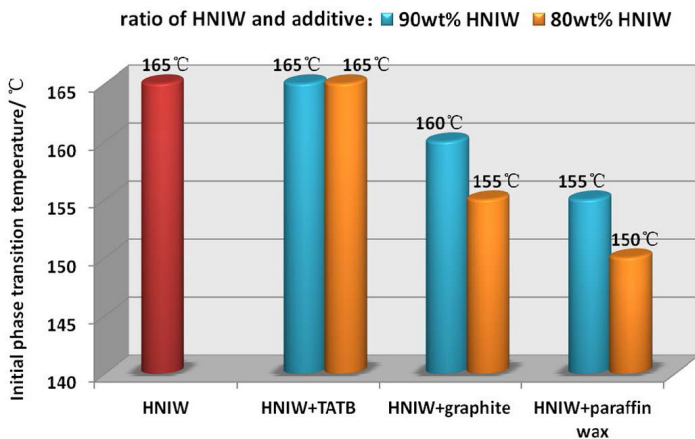


**Figure 6.** Initial phase transition temperatures of HNIW mixed with several insensitive additives.

With increasing content of graphite and paraffin wax, the initial phase temperature decreased correspondingly. The possible reason for this is that the presence of the impurity reduces the energy barrier of the phase transition, and the additive has additional heat and energy to induce the phase reconstruction.

Especially for paraffin wax with its low melting point and high conductivity of heat, the initial phase transition temperature is much lower than the others. By contrast, TATB is an inferior heat conductor. Moreover, TATB has a stable molecular structure and cannot provide extra contributions to the phase transition [38]. Thus, TATB is a good insensitive additive for HNIW in the formulation of composite explosives.

### 3.5 Influence of isothermal time on crystal structural transformation

The phase transition may occur under extended heat treatment due to the high energy provided to the HNIW. In order to verify structural changes in HNIW after different isothermal times, samples with the same properties as described in Section 3.4 were analyzed by *in-situ* PXRD. The samples were heated at  $0.1\text{ }^{\circ}\text{C}\cdot\text{s}^{-1}$  from ambient temperature to the target temperature, and were then scanned after 2 min at the constant temperature. XRD data were subsequently collected every 5 min for 4 h. The results are shown in Figure 7.

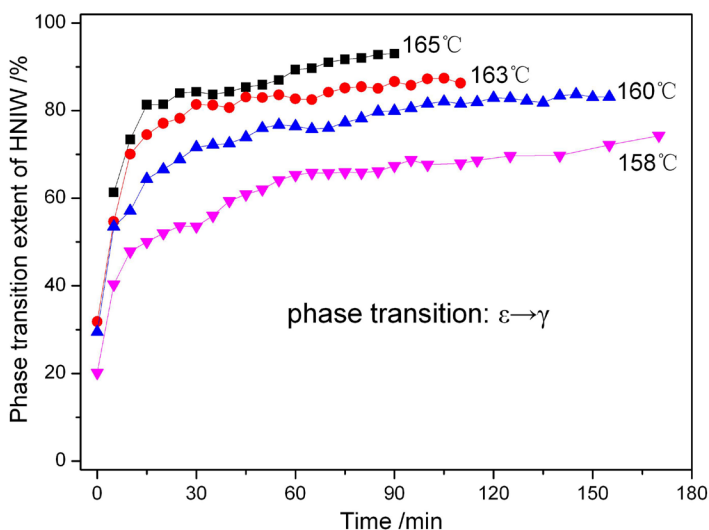


**Figure 7.** Increasing fraction of the  $\gamma$ -polymorph as a function of isothermal time: (■) heating temperature was  $165\text{ }^{\circ}\text{C}$ , (●)  $163\text{ }^{\circ}\text{C}$ , (▲)  $160\text{ }^{\circ}\text{C}$ , and (▼)  $158\text{ }^{\circ}\text{C}$ .

As shown in Figure 7, the effects of isothermal heating time were different at different temperatures. The weak diffraction peaks of  $\gamma$ -HNIW in the XRD patterns appeared above  $158\text{ }^{\circ}\text{C}$  after a certain time, indicating that the phase

transition of HNIW had occurred. The proportion of  $\gamma$ -HNIW increased with increasing isothermal time. Furthermore, the heating time required for phase transition decreased with increasing temperature. The new peaks occurred after only 2 min at 165 °C. If the isothermal time is long enough, complete phase transition can be achieved. In fact, there is a critical temperature for phase transition for every single sample. The phase transition can be realized by heating above that critical temperature for sufficient time. This point confirms that the occurrence of the phase transition of HNIW requires enough energy to overcome the barrier, to achieve the reconstruction of the internal structure, and to provide the additional energy to promote the crystal structural transformation [39].

## 4 Conclusions

The  $\varepsilon \rightarrow \gamma$  phase transition of HNIW on heating was investigated by *in-situ* PXRD. The phase transition of  $\varepsilon$ -HNIW occurred without complete destruction of the  $\varepsilon$ -phase. In the range of 150 °C to 180 °C, the two phases can coexist. Moreover, the phase transition is irreversible on cooling. The phase transition of  $\varepsilon$ - to  $\gamma$ -HNIW is related to the purity and particle size of the sample. The initial phase transition temperature increases with increasing purity and decreasing particle size of HNIW and thus with the approximate crystal density. The influence of different insensitive additives on the phase transition differs. The addition of graphite and paraffin wax to HNIW as insensitive additives leads to a decrease in the initial phase transition temperature, but the addition of TATB does not affect the initial phase transition temperature. Thus, TATB is a suitable insensitive additive. In addition, the isothermal time also affects the process of phase transition. The phase transition can be realized by heating above the critical temperature for sufficient time.

## Acknowledgements

This study was financially supported by the Nation Science Foundation, China (11372290, 11472252, 11572295, U1330202). We would like to thank Hongzhen Li for samples of the HNIW, and we also thank Ruijuan Xu and Minxia Zheng for helpful discussions related to the XRD and particle size measurements.

## References

- [1] Bernstein J., *Polymorphism in Molecular Crystals*, Oxford University Press, **2008**; ISBN 978-0-19-850605-8.
- [2] Blagden N., Davey R.J., Polymorph Selection: Challenges for the Future?, *Cryst. Growth Des.*, **2003**, 3(6), 873-885.
- [3] Xu J., Sun J., Zhou K., Shu Y., Review on Polymorphic Transformation of CL-20 in Recrystallization, *Chin. J. Energ. Mater.*, **2012**, 20(2), 248-255.
- [4] Xu J., Tian Y., Liu Y., Zhang H., Shu Y., Sun J., Polymorphism in Hexanitrohexaazaisowurtzitane Crystallized from Solution, *J. Cryst. Growth*, **2012**, 354, 13-19.
- [5] Russell T., Miller P., Piermarini G., Block S., Pressure/Temperature Phase Diagram of Hexanitrohexaazaisowurtzitane, *J. Phys. Chem.*, **1993**, 97(9), 1993-1997.
- [6] Zhang P., Xu J., Guo X., Jiao Q., Zhang J., Effect of Additives on Polymorphic Transition of  $\epsilon$ -CL-20 in Castable Systems, *J. Therm. Anal. Calorim.*, **2014**, 117, 1001-1008.
- [7] Xu J., Pu L., Liu Y., Sun J., Jiao Q., Guo X., Liu X., Polymorphic Transformation of  $\epsilon$ -CL-20 in Different HTPB-based Composite Systems, *Chin. J. Energ. Mater. (Hanneng Cailiao)*, **2015**, 23(2), 113-119.
- [8] Nielsen A.T., Chan M.L., Kraeutle C.K., *Polynitropolyazacaged Explosives*, Part 7. NWC TP 7200[R], China Lake: Naval Weapons Center, **1989**.
- [9] Nielsen A.T., *Caged Polynitramine Compound*, Patent US 5693794, **1997**.
- [10] Foltz M.F., Coon C.L., Garcia F., Nichols A.L., The Thermal Stability of the Polymorphs of Hexanitrohexaazaisowurtzitane, Part I, *Propellants Explos. Pyrotech.*, **1994**, 19(1), 19-25.
- [11] Foltz M.F., Coon C.L., Garcia F., Nichols A.L., The Thermal Stability of the Polymorphs of Hexanitrohexaazaisowurtzitane, Part II, *Propellants Explos. Pyrotech.*, **1994**, 19(3), 133-144.
- [12] Russell T., Miller P., Piermarini G., Nichols A.L., Block S., High-pressure Phase Transition in  $\gamma$ -Hexanitrohexaazaisowurtzitane, *J. Phys. Chem.*, **1992**, 96(13), 5509-5512.
- [13] Millar D.I.A., Maynard-Casely H.E., Kleppe A.K., Marshall W.G., Pulham C.R., Cumming A.S., Putting the Squeeze on Energetic Materials-Structural Characterization of a High-pressure Phase of CL-20, *CrystEngComm*, **2010**, 12(9), 2524-2527.
- [14] Ciezak J.A., Jenkins T.A., Liu Z., Evidence for a High-pressure Phase Transition of  $\epsilon$ -2,4,6,8,10,12-Hexanitrohexaazaisowurtzitane (CL-20) Using Vibrational Spectroscopy, *Propellants Explos. Pyrotech.*, **2007**, 32(6), 472-477.
- [15] Xu X., Zhu W., Xiao H., DFT Studies on the Four Polymorphs of Crystalline CL-20 and the Influences of Hydrostatic Pressure on  $\epsilon$ -CL-20 Crystal, *J. Phys. Chem. B*, **2007**, 111, 2090-2097.
- [16] Jin S., Shu Q., Chen S., Shi Y., Preparation of  $\epsilon$ -HNIW by a One-pot Method in Concentrated Nitric Acid from Tetraacetyldiformylhexaazaisowurtzitane,

- Propellants Explos. Pyrotech.*, **2007**, 32(6), 468-471.
- [17] Braithwaite P.C., Hatch R.L., Lee K., Wardle R.B., Mezger M., Nicolich S., Development of High Performance CL-20 Explosive Formulations, *29<sup>th</sup> Int. Annu. Conf. ICT*, Karlsruhe, **1998**, 4:1-5.
- [18] Bazaki H., Kawabe S., Miya H., Synthesis and Sensitivity of Hexanitrohexaazaisowurtzitane (HNIW), *Propellants Explos. Pyrotech.*, **1998**, 23(6), 333-336.
- [19] Lee M.H., Kim J.H., Park Y.C., Hwang J.H., Kim W.S., Control of Crystal Density of  $\epsilon$ -Hexanitrohexaazaisowurtzitane in Evaporation Crystallization, *Ind. Eng. Chem. Res.*, **2007**, 46, 1500-1504.
- [20] Löbbbecke S., Bohn M.A., Pfeil A., Krause H., Thermal Behavior and Stability of HNIW (CL-20), *29<sup>th</sup> Int. Annu. Conf. ICT*, Karlsruhe, **1998**, 145, 1-15.
- [21] Turcotte R., Vachon M., Kwok Q.S.M., Wang R., Jones D.E., Thermal Study of HNIW (CL-20), *Thermochim. Acta*, **2005**, 433, 105-115.
- [22] Thiboutot S., Brousseau P., Ampleman G., Pantea D., Cote S., Potential Use of CL-20 in TNT/ETPE-based Melt Cast Formulation, *Propellants Explos. Pyrotech.*, **2008**, 33(2), 103-108.
- [23] Hoffman D.M., Voids and Density Distributions in 2,4,6,8,10,12-Hexanitro-2,4,6,8,10,12-Hexaazaisowurtzitane (CL-20) Prepared under Various Conditions, *Propellants Explos. Pyrotech.*, **2003**, 28, 194-200.
- [24] Sun J., Shu X., Liu Y., Zhang H., Liu X., Jiang Y., Kang B., Xue C., Song G., Investigation on the Thermal Expansion and Theoretical Density of 1,3,5-Trinitro-1,3,5-triazacyclohexane, *Propellants Explos. Pyrotech.*, **2011**, 36, 341-346.
- [25] Mittemeijer E.J., Welzel U., *Modern Diffraction Methods*, John Wiley & Sons, **2013**; ISBN 978-3-527-32279-4.
- [26] Young R.A., *The Rietveld Method*, Oxford University Press, Oxford, **2002**; ISBN 0-19-855912-7.
- [27] Nielsen A.T., Chafin A.P., Christian S.L., Moore D.W., Nadler M.P., Nissan R.A., Vanderah D.J., Gilardi R.D., George C.F., Flippen-Anderson J.L., Synthesis of Polyazapolycyclic Caged Polynitramines, *Tetrahedron*, **1998**, 54, 11793-11812.
- [28] Cambridge Structure Database search, CSD Version 5.32, May **2011** update, Cambridge Crystallographic Data Centre, UK; [www.ccdc.cam.ac.uk](http://www.ccdc.cam.ac.uk).
- [29] TOPAS V3.0: *General Profile and Structure Analysis Software for Powder Diffraction Data*, Bruker AXS GmbH, Karlsruhe, **2000**.
- [30] Hugo M.R., The Rietveld Method (invited comment), *Phys. Scr.*, **2014**, 89, 1-6.
- [31] Hutton A.C., Mandile A.J., Quantitative XRD Measurement of Mineral Matter in Gondwana Coals Using the Rietveld Method, *J. Afr. Earth Sci.*, **1996**, 23(1), 61-72.
- [32] Zhang Z., Jiang C., Fu P., Cai F., Ma N., Microstructure and Texture of Electrodeposited Ni-ZrC Composite Coatings Investigated by Rietveld XRD Line Profile Analysis, *J. Alloys Compd.*, **2015**, 626, 118-123.
- [33] R ath S., Woodall L., Deroche C., Seipel B., Schwaigerer F., Schmahl W.W., Quantitative Phase Analysis of PBSCCO 2223 Precursor Powders – an XRD/Rietveld Refinement Study, *Supercond. Sci. Technol.*, **2002**, 15, 543-554.

- [34] Langer G., Eisenreich N., Hot Spots in Energetic Materials, *Propellants Explos. Pyrotech.*, **1999**, *24*, 113-118.
- [35] Bellamy A.J., A Simple Method for the Purification of Crude Hexanitrohexaazaisowurtzitane (HNIW or CL-20), *Propellants Explos. Pyrotech.*, **2003**, *28*, 145-151.
- [36] Diao Y., Allan S.M., Hatton T.A., Trout B.L., Surface Design for Controlled Crystallization: the Role of Surface Chemistry and Nanoscale Pores in Heterogeneous Nucleation, *Langmuir*, **2011**, *27*, 5324-5334.
- [37] Hu Q., Lu Z., Study of Desensitizing Effect of TATB, Wax and Graphite, *Chin. J. Energ. Mater.*, **2004**, *12*(1), 26-29.
- [38] Zhang C., Wang X., Huang H.,  $\pi$ -Stacked Interactions in Explosive Crystals: Buffers Against External Mechanical Stimuli, *J. Am. Chem. Soc.*, **2008**, *130*(26), 8359-8365.
- [39] Li J., Brill T.B., Kinetics of Solid Polymorphic Phase Transitions of CL-20, *Propellants Explos. Pyrotech.*, **2007**, *32*(4), 326-330.